

N93-14392

**LOW-EMISSIVITY IMPACT CRATERS ON VENUS.** C. M. Weitz<sup>1</sup>, C. Elachi<sup>1</sup>, H. J. Moore<sup>2</sup>, A. T. Basilevsky<sup>3</sup>, B. A. Ivanov<sup>4</sup>, and G. G. Schaber<sup>5</sup>, <sup>1</sup>Jet Propulsion Laboratory, California Institute of Technology, Pasadena CA 91109, USA, <sup>2</sup>USGS, Menlo Park CA 94025, USA, <sup>3</sup>Vernadsky Institute of Geochemistry and Analytical Chemistry, Russian Academy of Sciences, Moscow, 117975, Russia, <sup>4</sup>Institute for Dynamics of Geospheres, Russian Academy of Sciences, Moscow, 123810, Russia, <sup>5</sup>USGS, Flagstaff AZ 86001, USA.

**Procedure:** An analysis of 144 impact craters on Venus has shown that 11 of these have floors with average emissivities lower than 0.8. The remaining craters have emissivities between 0.8 and 0.9, independent of the specific backscatter cross section of the crater floors. These 144 impact craters were chosen from a possible 164 craters with diameters greater than 30 km as identified by Schaber et al. [1] for 89% of the surface of Venus. We have only looked at craters below 6053.5 km altitude because a mineralogical change causes high reflectivity/low emissivity above this altitude [2]. We have also excluded all craters with diameters smaller than 30 km because the emissivity footprint at periaapsis is 16 × 24 km and becomes larger at the poles [3].

On the SAR images, rectangular boxes were chosen on the crater floor that avoided central peaks and inner rings. Backscatter cross sections were calculated from the average DN values within the boxes for the incidence angle for the crater latitude. Emissivity values were taken from the datasets produced by MIT [3]. A rectangular box was selected inside each crater floor and the average DN was then converted to emissivity. In Fig. 1, while the majority of crater floors lie between 0.8 and 0.9 in average emissivity independent of backscatter cross sections, 11 craters fall below this range.

We also found all craters that had any emissivity values on their floors below or equal to 0.8 because several craters had variations across their floors. After doing this, we found five more crater floors with emissivity values below or equal to 0.8. Table 1 lists the 16 craters and the lowest emissivity values found on their floors. The 16 craters represent a minimum number of craters with low emissivities on Venus because craters with diameters smaller than the footprint of the radiometer may have low emissivities that will not be detected.

**Results:** A study of backscatter and emissivity for impact craters associated with parabolic-shaped features by Campbell et al. [4] indicates that the majority of these craters have high specific

The observation that rms slopes obtained from direct inversion of the altimetry data are consistent, at least in a general way, with values derived from template fits [1] provides some confidence that both these procedures are reliable. Since the recovered functions from inversion  $\hat{\sigma}_0(\phi)$  do not depend on *a priori* specification of an analytic function, we expect to find differences between our results and those obtained via the template method as our analysis proceeds.

Our result that an exponential scattering function can provide better agreement with data than the widely used Hagfors function is significant in terms of its implications for the surface. Although the difference is not large, it is convincing. A gaussian surface model is derived by assuming that the surface is gently rolling. A Hagfors surface must have at least a few flat segments and some "edges" in order to justify use of an exponential autocorrelation function. The degree to which a fresh planetary surface has been turned over and smoothed may be expressed in the degree to which its scattering is described by gaussian functions rather than Hagfors functions. The exponential function requires that there be more or larger flat-lying segments than even the Hagfors function requires. We note that while the exponential law works best for Venus, just the opposite is the case for the Moon [2]. It seems likely this difference reflects underlying differences in processes of erosion and deposition and of materials on the two bodies.

Our results from SAR image analysis to date are limited. We have found a smooth region (in altimetry data) east of Alpha Regio where SAR backscatter cross section is lower than predicted by the Muhleman function, suggesting that the same scattering mechanisms apply at both nadir and at  $\phi \approx 30^\circ$  and  $35^\circ$ . East of Maxwell, SAR backscatter is above average, but our estimates of rms slopes and those derived from template fitting [3] indicate that this is an "average" region in its nadir backscatter. The difference could be accounted for by the presence of small-scale roughness that is not apparent to the altimeter but scatters relatively strongly at oblique angles.

The Doppler offset observations appear to be real and a manifestation of a geophysical or geological state of the surface. They show global patterns that include a great circle at equatorial latitudes (roughly following the band of equatorial highlands that includes Aphrodite Terra, Eistla Regio, and Beta Regio) and at least part of another (constant latitude) circle at  $40^\circ$ – $50^\circ$  N. Large-scale surface slopes from Pioneer Venus topography [4] correlate to some extent, but are inadequate by themselves to cause the displacements observed. Small-scale "shingles" or other asymmetric scattering surfaces (for example, sand dunes [R. A. Arvidson, personal communication]) could contribute, but acquiring independent confirming data will be difficult. Local slopes of  $0.3^\circ$  on kilometer scales may also be important [P.G. Ford, personal communication], but more needs to be learned of their distribution. A concentration of negative offsets between Sapas Mons and Rusalka Planitia, where the large-scale surface gradient is perpendicular to the Magellan track, indicates that this phenomenon need not be associated with large-scale slopes. Global-scale "zones of disruption" [5] may have led to surface modification, which is expressed in small-scale surface features but does not necessarily show up in the large-scale topography.

**References:** [1] Ford P. G. and Pettengill G. H. (1992) *JGR*, submitted. [2] Simpson R. A. and Tyler G. L. (1982) *IEEE Trans.*, AP-30, 438–449. [3] Tyler G. L. et al. (1991) *Science*, 252, 265–270. [4] Sharpton V. L. and Head J. W. (1985) *JGR*, 90, 3733–3740. [5] Schaber G. G. (1982) *GRL*, 9, 499–502.

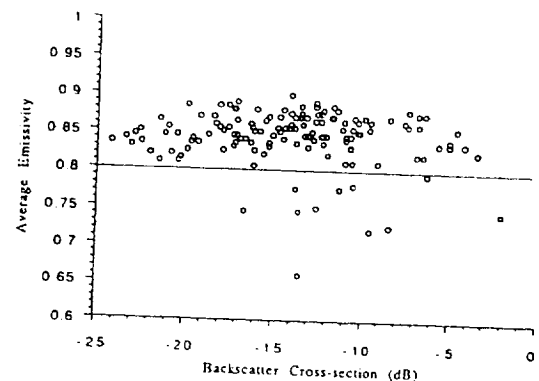


Fig. 1. Emissivity and specific backscatter cross section for 144 craters on Venus.

TABLE 1. Data on 16 craters with floors that have low emissivities.

Crater	Latitude	Longitude	Diameter (km)	Backscatter cross section (dB)	Emissivity
Boleyn	24.4	219.9	70	-13.52	0.62
Stanton	-23.4	199.9	110	-9.53	0.665
Stuart	-30.75	20.2	71	-8.45	0.69
Mead	12.5	57.2	280	-16.64	0.705
Adivar	8.95	76.1	32	-13.64	0.715
Sitwell	16.68	190.35	37	-12.64	0.72
Stowe	-43.2	233	80	-2.07	0.725
Warren	-11.8	176.5	53	-13.78	0.735
Truth	28.7	287.75	49	-11.25	0.745
Greenaway	22.95	145	92	-10.52	0.755
Boulanger	-26.55	99.3	73	-6.31	0.76
Bonheur	9.8	288.75	109	-13.84	0.775
Aurelia	20.25	331.85	32	-10.98	0.785
Ban Zhao	17.2	146.9	40	-10.64	0.785
O'Keefe	24.5	228.75	81	-16.12	0.79
Bathsheba	-15.1	49.35	35	-9.1	0.8

radar backscatter cross sections and low emissivities. They suggest that these craters are relatively young and that these radar-bright floors are the result of wavelength scale roughness and high Fresnel reflectivity material. With time, modification processes remove the parabolic deposits and alter the crater floors to lower backscatter cross sections, lower Fresnel reflectivities, and higher emissivities that match those typical of the older craters without parabolic features.

We have plotted the specific backscatter cross sections for the 144 craters used in our analysis (Fig. 2). The dashed line is the Muhleman Law, which is the derived average scattering function based on Pioneer Venus SAR observations and used by the Magellan project to normalize the backscatter cross sections. Because all but one (Mead) of the low-emissivity crater floors have stronger backscatter than most craters, this supports an association between low-emissivity and high-backscatter cross sections for most craters on Venus. Of these 16 low-emissivity craters, 7 are peak ring, 6 are central peak, and 3 have no floor structure. Ten of these craters have associated parabolic features.

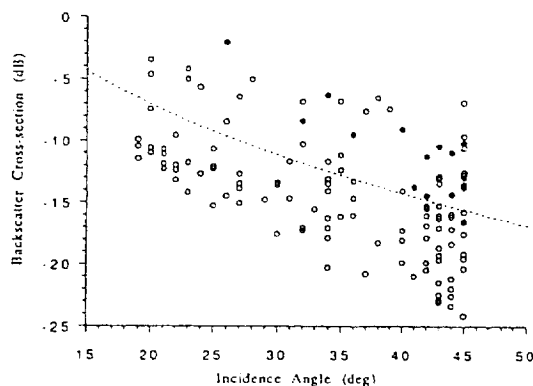


Fig. 2. Specific backscatter cross section vs. incidence angle for 144 craters on Venus. Dashed line is the Muhleman Law. Filled circles are low-emissivity craters, open circles high-emissivity craters.

**Interpretations:** To help us interpret the materials in the crater floors, we have used a relation between bulk density and relative dielectric constant for lunar samples of rocks and "soils" [5]. A Fresnel reflectivity near 0.38 can be inferred [3] from the emissivity (0.62) of crater floor materials of Boleyn (Table 1) to yield a calculated dielectric constant of 17.8 [6]. The inferred bulk density, which is  $4380 \text{ kg/m}^3$  (range: 3880–5090), is much too large for common basaltic rocks. More probable bulk densities of basaltic rocks, which have dielectric constants near 8 to 9 [7], lie in the range of 2600–3000  $\text{kg/m}^3$ .

Low emissivity values for the venusian highlands can best be explained by the presence of conducting minerals, such as iron pyrite, iron sulfides, or iron oxides [8]. We also suggest that inclusions of conducting minerals or particles in the crater floor materials could account for the low emissivities and high Fresnel reflectivities. Materials containing these particles may have been (1) excavated from depth in the crust during the impact process, (2) derived from the projectile that produced the crater, (3) formed by physical-chemical reactions associated with the impact process (including impact melts), (4) extruded into the crater by volcanic processes, and (5) produced by some combination of these processes. The absence of low-emissivity signatures on the crater flanks and bright outflows suggest that 1, 2, and 3 are unlikely because the low emissivities are confined to crater floors. It may be possible, however, that atmospheric shocks associated with the impacts confine materials or impact metamorphism is confined to the materials of the floors.

Some of the craters are clearly filled with postcrater lavas while others may be filled with impact melts. In the case of the crater Bonheur, the flooded interior basin has a lower emissivity and a smaller backscatter cross section than the outer basin. This observation supports an endogenous lava flow with low emissivity (possibly high in iron content) that has flooded the interior basin. Two low-emissivity craters reside on the tessera and one of these appears to be partly flooded by lava. This means that low emissivity lavas may erupt from magma sources beneath the tessera as well as the plains. Backscatter cross sections for both the floors and outflows of some craters, such as Stowe, are about the same and this suggests the materials of the floors include impact melts. The next step is to investigate how this low-emissivity material could weather to the

higher emissivity values (0.8–0.9) on the plains and on the other crater floors and to investigate whether young lava flows also exhibit low emissivities. (This work was conducted at the Jet Propulsion Laboratory, California Institute of Technology, under contract with the National Aeronautics and Space Administration.)

**References:** [1] Schaber et al. (1992) *JGR*, in press. [2] Klose et al. (1992) *JGR*, in press. [3] Pettengill et al. (1991) *Science*, 252, 260–265. [4] Campbell et al. (1992) *JGR*, in press. [5] Olhoeft G. R. and Strangway D. W. (1975) *EPSL*, 24, 394–404. [6] Tyler et al. (1976) *Science*, 193, 812–815. [7] Campbell M. J. and Ulrichs J. (1969) *JGR*, 74, 5867–5881. [8] Pettengill et al. (1988) *JGR*, 93, 14881–14892.

**N93-14393**

**FLOOR-FRACTURED CRATER MODELS FOR IGNEOUS CRATER MODIFICATION ON VENUS.** R. W. Wichman and P. H. Schultz, Department of Geological Sciences, Brown University, Providence RI 02912, USA.

**Introduction:** Although crater modification on the Earth, Moon, and Mars results from surface erosion and crater infilling, a significant number of craters on the Moon also exhibit distinctive patterns of crater-centered fracturing and volcanism that can be modeled as the result of igneous crater modification [1–5]. Here, we consider the possible effects of Venus surface conditions on this model, describe two examples of such crater modification, and then briefly discuss the constraints these craters may place on conditions at depth.

**Floor-fractured Crater Model:** On the Moon, most floor-fractured craters occur near the lunar maria [1,6,7] or along basin ring faults [5], and commonly contain ponded mare units and dark mantling deposits [1,8,9]. Fracturing is confined to the crater interior, and, in the more modified craters, uplift of the crater floor as a single coherent unit results in a distinctive moatlike failure zone in the crater wall region [1,4]. In some cases, later volcanism floods this moat structure or buries the entire floor [1,3].

Although viscous relaxation can produce uplift of the crater floor [10–12], shallow, laccolithlike intrusion beneath the crater floor provides a model consistent with observations on the Moon. As discussed elsewhere [1,4,5], intrusions apparently begin in a neutral buoyancy zone near the base of the crater-centered breccia lens through the lateral growth of a sill-like magma body. Both the increased lithostatic pressures and diminished impact brecciation beneath the crater walls, however, enhance resistance to such lateral intrusion growth beyond the crater floor region, thereby evolving into vertical, laccolithic intrusion growth described by [13]. During vertical growth, the crater floor rises through a pistonlike uplift, while ring faulting near the edge of the intrusion produces the moat structures outside this uplift.

For a laccolithic intrusion, crater modification is controlled by parameters that allow assessing conditions at depth [4,5]. Since elastic deformation should not thin the uplifted crater floor section, the amount of floor uplift essentially reflects the intrusion thickness. If the uplifted floor diameter delineates the laccolith size at depth, then the model [13] can be used to estimate both the magma pressure driving deformation and an effective thickness for the crater floor materials overlying the intrusion. The derived magma pressures then help constrain the length of the magma column beneath the intrusion, whereas the inferred floor thickness provides a model for both the intrusion depth and breccia thickness in a given crater [4,5].

**Floor-fractured Craters on Venus:** The evidence for widespread volcanism on Venus [14] would seem to favor igneous crater

modification. Four significant differences between conditions on Venus and on the Moon may modify the processes of crater-centered igneous intrusion. First, where the anorthositic crust on the Moon is apparently equivalent in density or less dense than most mare magmas [15], the basaltic crust on Venus should be denser than basaltic melts and may be thinner than the lunar crust as well. Consequently, basalt magmas on Venus are more likely to rise to the surface than magmas on the Moon, perhaps decreasing the likelihood of crater-centered intrusions at depth [4]. Second, the lunar crust has been extensively fractured by successive, overlapping impact events. The resulting combination of a megaregolith and basin ring faults, therefore, provides a number of conduits through which magma can enter individual crater-centered breccias. In contrast, the crust on Venus appears to be more coherent; hence, magma may not favor breccias beneath craters on Venus. Instead, a crater-centered intrusion may first require deformation by a regional fracture system. Third, the higher surface gravity on Venus should reduce the fracture porosity of an impact breccia, thereby reducing the density contrast required for a shallow zone of crater-centered neutral buoyancy. High surface gravity also should consolidate impact breccias at depth, which may produce thinner breccia lenses on Venus than on the Moon. As a result, the uplifted floor plate on Venus should be thinner than on the Moon, and floor fracturing would then be expected to be more polygonal, i.e., reflecting inhomogeneities in the floor rather than acting as a coherent block. Fourth, since the increased surface temperatures on Venus may allow annealing of impact breccias over time, both the fracture density beneath a Venus crater and the probability of an igneous intrusion also may decrease as a function of crater age.

Most impact craters on Venus do not exhibit floor fractures comparable to examples on the Moon. Instead, either volcanic infilling occurs or craters are simply engulfed rather than participate in surface volcanism. Figures 1 and 2, however, illustrate two craters that closely resemble floor-fractured craters on the Moon. For reference, both craters occur in ridged lowland plains with elevations of approximately –500 m to 500 m, relative to the mean planetary radius. The first of these craters (Fig. 1) is 48 km in diameter and exhibits a scarp-bounded central floor plate 32 km in diameter in which an additional pattern of concentric failure can be



Fig. 1. Modified crater centered at 52°S, 196°E. Note the wide outer moat structure surrounding the central floor and the bright scarp along the southwest edge of the central floor plate. Scale bar is ~17 km (enlarged section of C1-45S202; 1).